ELECTRON CLOUD MITIGATION INVESTIGATIONS AT CESR-TA*

J.R. Calvey, J. Makita, M.A. Palmer, R.M. Schwartz,
C.R. Strohman, CLASSE, Cornell University, Ithaca, NY, USA
S. Calatroni, G. Rumolo, CERN, Geneva, Switzerland
K. Kanazawa, Y. Suetsugu, KEK, Ibaraki, Japan†
M. Pivi, L. Wang, SLAC, Menlo Park, CA, USA

Abstract

As part of an effort to understand and mitigate the electron cloud effect, the CESR storage ring at Cornell has been reconfigured into a damping ring-like setting, as well as instrumented with a large number of electron cloud diagnostic devices. In particular, more than 30 Retarding Field Analyzers (RFAs) have been installed. These devices, which measure the local electron cloud density and energy distribution, have been deployed in drift, dipole, quadrupole, and wiggler field regions, and have been used to evaluate the efficacy of cloud mitigation techniques in each element.

INTRODUCTION

The density, energy distribution, and transverse profile of the electron cloud can depend strongly on several parameters that can vary substantially throughout an accelerator. These include local photon flux, vacuum chamber shape and material, primary and secondary emission properties of the material, and magnetic field type and strength. Therefore it is useful to have a detector that can sample the electron cloud locally. At CesrTA we have primarily used Retarding Field Analyzers (RFAs) for this purpose [1]. RFAs can measure the energy distribution of the cloud by applying a retarding potential between two grids, rejecting any electrons below a certain energy[2]. In addition, most RFAs are segmented across the top of the beam pipe, effectively measuring the transverse distribution of the cloud.

We have used these devices to probe the local behavior of the cloud in the presence of different mitigation schemes. Several such schemes have been proposed, including beam pipe coatings (TiN, amorphous Carbon, NEG) [3, 4], grooved beam pipes [5], solenoids, and clearing electrodes [6].

Table 1 provides a list of the mitigation techniques that have been evaluated so far at CesrTA.

DRIFT MEASUREMENTS

Fig. 1 shows a typical retarding voltage scan in an TiN coated drift chamber for a 45 bunch train of positrons, at 1.25 mA/bunch (corresponding to a bunch population of 2×10^{10}), 14ns spacing, and beam energy 5.3 GeV. The plot

Table 1: Mitigation techniques at CesrTA

Field Type	Base Material	Mitigation
Drift	Aluminum, Copper	TiN, Carbon, NEG coatings, solenoids
Dipole	Aluminum	TiN coating, grooves
Quadrupole	Aluminum	TiN coating
Wiggler	Copper	TiN coating, grooves, clearing electrode

shows the RFA response as a function of collector number and retarding voltage. The RFA signal is expressed in terms of current density in nA/mm^2, normalized to the transparency of the RFA beam pipe and grids. In principle, this gives the time averaged electron current density incident on the beam pipe wall. The signal is peaked at low energy and in the central collectors, though some current remains at high energy in the central collectors and at low energy in all collectors.

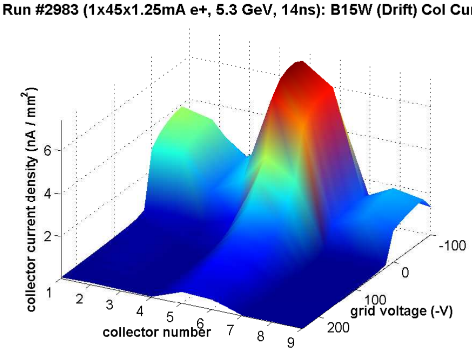

Figure 1: Example voltage scan: TiN coated drift RFA

We have taken RFA data in both TiN and amorphous Carbon coated drift chambers, as well as an uncoated Aluminum chamber. All three of these chambers have been installed at the same location in the ring at different times. This ensures that the comparison is done with the exact same beam conditions, including photon flux and beam size.

A comparison of different beam pipe coatings in a drift region can be found in Fig. 2. It shows the average collector current density as a function of beam current (in this case

* Work supported by the US National Science Foundation (PHY-0734867) and Department of Energy (DE-FC02-08ER41538)
† Work supported by The Japan/US Cooperation Program

for a 20 bunch train of positrons), for all of the chamber coatings mentioned. There are two sets of data shown for the TiN chamber, one taken shortly after it was installed, and one taken after four months of beam processing. The Carbon chamber did not show significant processing.

Both TiN and Carbon coatings show a largely suppressed signal relative to Aluminum. The Carbon chamber falls in between unprocessed and processed TiN.

Fig 3 shows the same comparison for data taken with an electron beam. Though the scale is smaller on this plot, the relative performance of the three chamber types is roughly the same.

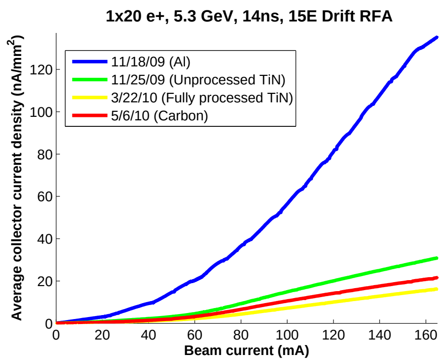

Figure 2: Drift RFA comparison, positron beam

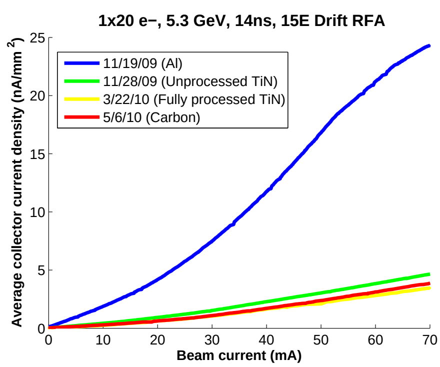

Figure 3: Drift RFA comparison, electron beam

NEG Coated Chamber

We have also installed a NEG coated chamber in our L3 straight region. This chamber is instrumented with three single collector RFAs, located at different azimuthal positions. Fig. 4 shows the current measured by one of these RFAs, comparing the signal before activation of the NEG, after activation, and after processing. Both activation and processing reduce the current measured by this RFA; the other two detectors behave similarly.

DIPOLE MEASUREMENTS

Most of our dipole RFA measurements were done using a chicane of four magnets built at SLAC [7]. The

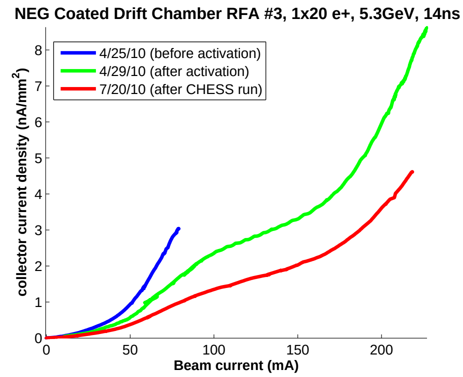

Figure 4: NEG RFA comparison

field in these magnets is variable, but most of our measurements were done in a nominal dipole field of 810G. Of the four chicane chambers, one is bare Aluminum, two are TiN coated, and one is both grooved and TiN coated. The grooves are triangular with a depth of 5.6mm and an angle of 20°. A retarding voltage scan, done in the Aluminum chamber and with the same beam conditions as Fig. 1, can be seen in Fig. 5. Here one can see a strong central multipacting spike.

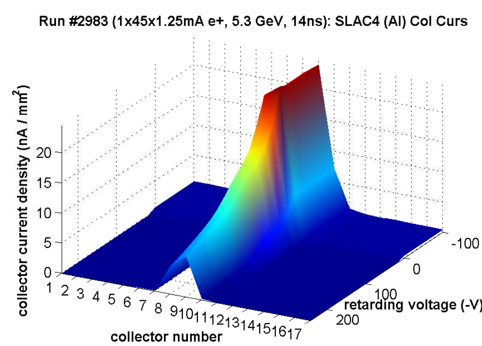

Figure 5: Typical dipole RFA measurement

Fig. 6 shows a comparison between three of the chicane RFAs. We found the difference between uncoated and coated chambers to be even stronger than in a drift region. At high beam current, the TiN coated chamber shows a signal smaller by two orders of magnitude than the bare Al chamber, while the coated and grooved chamber performs better still.

Bifurcation

For high bunch currents, one actually observes a bifurcation of the central multipacting peak into two peaks with a dip in the middle. This is demonstrated in Fig 7, which shows the signal in all 17 RFA collectors vs beam current. Bifurcation occurs when the average energy of electrons in the center of the beam pipe is past the peak of the SEY curve, so that the effective maximum yield is actually off

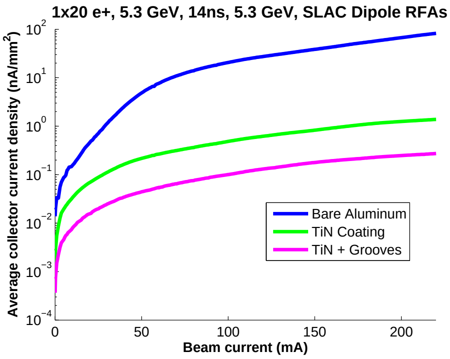

Figure 6: Dipole RFA comparison

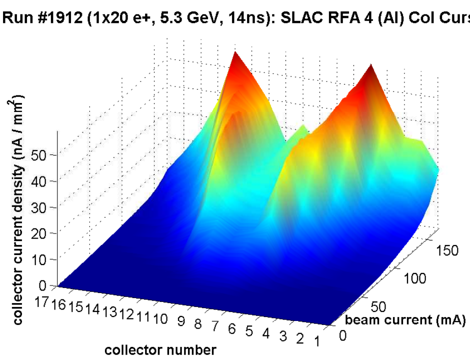

Figure 7: Bifurcation of peak density in a dipole

center. The higher the bunch current, the further off center these peaks will be.

QUADRUPOLE MEASUREMENTS

Another development at CesrTA has been the incorporation of an RFA into a quadrupole chamber. This RFA wraps azimuthally around the chamber, from about 70 to 150 degrees (taking zero degrees to be the source point). A typical quadrupole RFA measurement is shown in Fig. 8. We find that the collector that is lined up with the quad pole tip (no. 10) sees a large amount of current, while the rest of the collectors see relatively little. This suggests that the majority of the cloud in the quad is streaming between two pole tips.

Fig. 9 shows a comparison of a bare Aluminum (both processed and unprocessed) quadrupole chamber with the TiN coated chamber that has replaced it. In this comparison only collector 10 is being plotted. The signal in the TiN chamber was found to be reduced by well over an order of magnitude.

Long Term Cloud Trapping

One potential side effect of the cloud mirroring between the quad pole tips is that it may become trapped for a long time. We have seen some evidence of this at CesrTA. Fig 10 shows the signal in collector no. 10 for a voltage scan done with a 45 bunch train of positrons at 1mA/bunch. Also

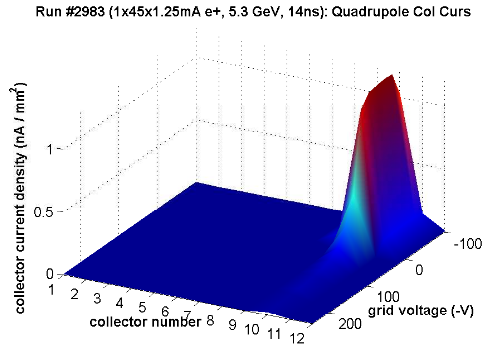

Figure 8: Quadrupole RFA measurement

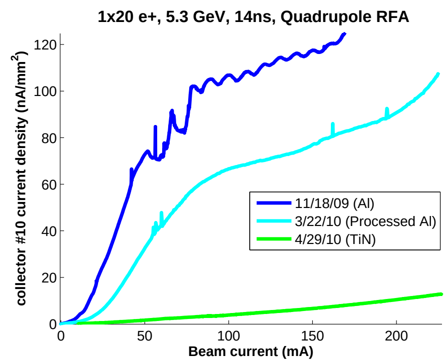

Figure 9: Quadrupole mitigation comparison

plotted are simulations done in ECLOUD [8] of these conditions. If one does a simulation for only one beam revolution period (2.56μs), the simulated signal is too low at all energies by over an order of magnitude. However, if one continues the simulation for multiple turns of the beam, one finds that the data and simulation start to get closer. By 19 turns, they are in very good agreement at high energy, and within a factor of 2 at low energy. This implies that the cloud is building up over several turns, and that the RFA is sensitive to this slow buildup.

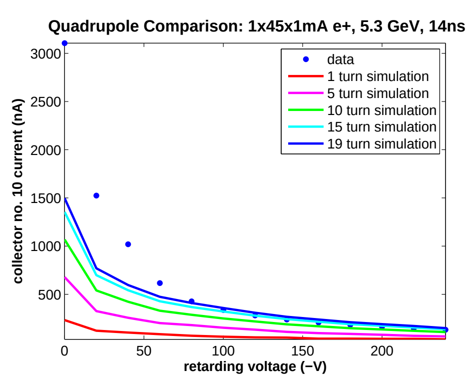

Figure 10: Long term cloud buildup in a quadrupole

WIGGLER MEASUREMENTS

The L0 straight section of CESR has been reconfigured to include six superconducting wigglers, three of which are instrumented with RFAs [9]. Each wiggler has an RFA in the center of one of the wiggler poles (where the transverse field is largest), half way between poles (where the field is longitudinal), and in an intermediate region. This paper will focus on the center pole RFA, which can roughly be considered to be in a 1.9T dipole field.

Fig. 11 shows a typical Cu wiggler RFA voltage scan for a 45 bunch train of positrons at 1.25mA/bunch, 14ns spacing, and 2.1 GeV. The signal is fairly constant across all the collectors at low retarding voltage, but does become peaked at the center at high energy. There is also an anomalous spike in current at low (but nonzero) retarding voltage; we believe this is due to a resonance between the bunch spacing and retarding voltage [10].

As with the drift RFAs, cycling the location of the different wigglers has allowed us to compare the RFA response with different mitigation techniques in the same longitudinal position in the ring. We have tested chambers with bare Copper, TiN coating, triangular grooves (with no coating, 2mm depth and 20° angle), and a clearing electrode. Fig. 12 shows the average collector current vs beam current in three chambers with mitigation; the copper wiggler is adjacent to this location, and is shown for a rough comparison. Note that, unlike the other measurements presented so far in this paper, beam pipe coating does not appear to lead to a significant reduction in RFA current, and grooves lead only to a small improvement. The chamber instrumented with a clearing electrode, however, shows a sizable reduction in signal. The electrode was set to 400V for this measurement.

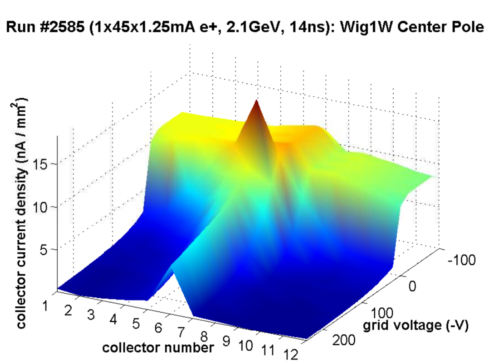

Figure 11: Wiggler RFA measurement, Cu chamber

Wiggler Ramp

Another interesting measurement that has been done with our wiggler RFAs is a "wiggler ramp", in which the RFA signal is monitored while the field in all six wigglers is ramped down from full (1.9T) to zero. Fig. 13 shows the signal in our three center pole wiggler RFAs vs wiggler field. We observe a "turn on" of the signal in each detector at a specific wiggler field value. Note that the detectors that are further downstream (i.e. have a higher s value) turn on first. This is because as the wiggler field in increased, the radiation fan becomes wider, and photons generated by the wiggler will collide with the beam pipe wall sooner. The farther downstream a detector is, the less wide the fan must be for photons to hit at that location. This measurement can help us understand the scattering properties of photons generated in this region, since only photoelectrons produced on the top or bottom of the beam pipe will be detectable by the RFA.

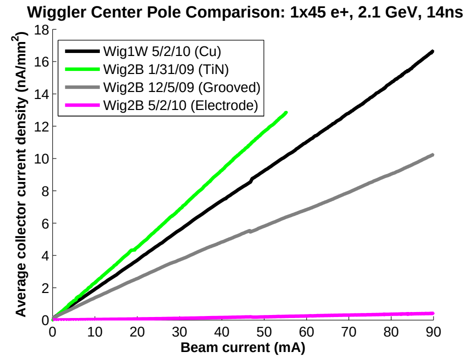

Figure 12: Wiggler mitigation comparison

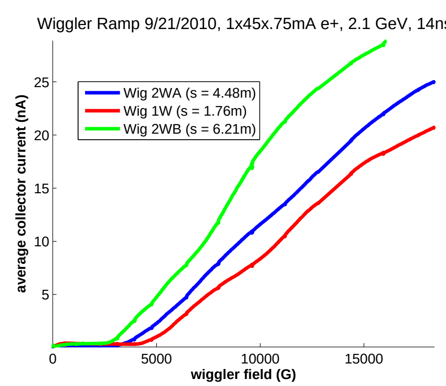

Figure 13: Wiggler ramp measurement

CONCLUSIONS

A great deal of RFA data has been taken at CesrTA, in a wide variety of beam conditions and magnetic field elements. Many interesting phenomena have been observed, including bifurcation of the peak density in a dipole, long term cloud trapping in a quadrupole, and a resonance with retarding voltage in a wiggler.

In terms of the effectiveness of mitigation types, several qualitative comments can be readily made:

- We have found beam pipe coatings (TiN, Carbon, and NEG) to be effective at mitigating the cloud in drifts.

- TiN coating was also found to be effective in a dipole and quadrupole; using a grooved and coated chamber in a dipole is even more effective.
- In a wiggler, a clearing electrode appears to be the most effective mitigation technique.

A systematic study to obtain more quantitative information about the different chambers, in particular their primary and secondary electron yield properties, is currently underway [11].

REFERENCES

[1] M. Palmer et. al., PAC09, Vancouver, TH5RFP030

[2] R.A. Rosenberg, K.C. Harkay, Nucl. Instrum. Meth. A 453, 507 (2000).

[3] E. Shaposhnikova et. al., PAC09, Vancouver, MO6RFP008

[4] F. Le Pimpec et. al., http://arxiv.org/abs/physics/0405098v1

[5] L. Wang, T. O. Raubenheimer and G. Stupakov, NIM-PR-A, 571, 588 (2007).
M. Pivi, F. K. King, R. E. Kirby, T. O. Raubenheimer, G. Stupakov and F. Le Pmpec, J. Appl. Phys., 104, 104904 (2008).

[6] Y. Suetsugu, H. Fukuma, L. Wang, M. T. F. Pivi, A. Morishige, Y. Suzuki, M. Tsukamoto, NIM-PR-A, 598, 372.

[7] M. T.F. Pivi, J. S.T. Ng et al. Nucl. Instr. Methods A, doi:10.1016/j.nima.2010.04.052.

[8] F. Zimmermann and G. Rumolo, ICFA Beam Dynamics Newsletter No. 33, eds. K. Ohmi and M.A. Furman (2004).

[9] Y. Li et. al., PAC09, Vancouver, TH5RFP029.

[10] J. Calvey et. al., IPAC10, Kyoto, TUPD022.

[11] J. Calvey et. al., “Methods for Quantitative Interpretation of Retarding Field Analyzer Data”, these Proceedings.